JACC Vol. 27, No. 7
June 1996:1753–60

REVIEW ARTICLE

A Practical Guide to Assessment of Ventricular Diastolic Function Using Doppler Echocardiography

GERALD I. COHEN, MD, FACC, JOSEPH F. PIETROLUNGO, DO, FACC,*
JAMES D. THOMAS, MD, FACC,* ALLAN L. KLEIN, MD, FACC*
Detroit, Michigan and Cleveland, Ohio

Doppler assessment of diastolic function has become a standard part of routine echocardiographic examination and imparts information relevant to a patient's functional class, management and prognosis. This review describes the Doppler patterns of diastolic function relative to physical signs and physiology. A continuum of Doppler patterns of diastolic function exists, including normal diastolic function, impaired relaxation, pseudonormal filling, restriction, constriction and tamponade. These patterns evolve from one to another in a single individual, with changes in disease evolution, treatment and loading conditions. New applications of continuous wave Doppler, color Doppler M-mode and Doppler tissue imaging are refining our understanding of diastolic function.

(J Am Coll Cardiol 1996;27:1753–60)

Doppler echocardiography is an important tool in the care of patients with heart failure. It provides a noninvasive, safe and rapid bedside alternative to cardiac catheterization for the assessment of ventricular diastolic function (1). Although absolute pressures are never directly measured, Doppler demonstration of blood flow direction and velocity corresponds to direct hemodynamic pressure recording (2–6) and measurement of left ventricular diastolic pressure (7–10). By detecting differences in diastolic function in patients with similar two-dimensional echocardiographic findings, Doppler distinguishes pathophysiologic entities and indicates functional class and prognosis (11–15). The goal of this report is to provide the clinician with a practical review of the Doppler patterns of diastolic function, as well as their current and future applications.

Standard Doppler Measurements

Ventricular inflow. The Doppler measurements of diastolic function are the product of atrial and ventricular relaxation, contraction (16–18), compliance and loading (2,19–22). Analogous flows are recorded from both sides of the heart. At the onset of diastole, the isovolumetric relaxation time occurs between the Doppler sounds of aortic valve closure and mitral valve opening (8). When the mitral and tricuspid valve open, blood inflow velocity accelerates to a peak early filling velocity, which coincides with the third heart sound (23). With ventricular filling, inflow velocity decelerates at a measurable rate called the *deceleration time*. Subsequent atrial contraction causes the late filling velocity, which begins with the onset of the fourth heart sound (Fig. 1A, B) (23).

Atrial inflow. Flow in the pulmonary and hepatic veins has two intervals of forward flow and one or two intervals of flow reversal (Fig. 1C, D) (18,24,25). During ventricular systole, descent of the base (16,18) and atrial relaxation (17,26) are associated with venous forward flow into the atria. Coinciding with the *x descent* of the venous pressure tracing (27), this flow increases to a peak systolic velocity and then falls, sometimes to the point of flow reversal, as atrial filling and pressure rise (25,28).

With mitral and tricuspid valve opening, the atria empty, atrial pressure falls and venous forward flow resumes until a peak diastolic filling velocity is achieved, which occurs at the time of the venous pressure *y descent* (27). As ventricular and atrial filling and pressures rise, venous return falls. At end-diastole, atrial contraction ejects blood back into the veins and causes venous flow reversal, in addition to augmenting ventricular filling. How much atrial blood goes forward or backward depends on the systolic function and loading conditions of the contracting atrium (2,7,19,22,29).

Patterns of Diastolic Function

Normal function. Table 1 lists normal Doppler reference values (28,30). Filling is progressively delayed in the aging ventricle as myocardial relaxation slows and wall thickness increases. This is manifested by an increased A wave velocity, deceleration time and isovolumetric relaxation time and an early transmitral flow velocity to atrial flow velocity (E/A) velocity ratio <1 (28,30,31). Aging is associated with increased

From the Sinai Hospital, Detroit, Michigan; and *The Cleveland Clinic Foundation, Cleveland, Ohio.

Manuscript received July 6, 1995; revised manuscript received February 9, 1996, accepted February 14, 1996.

Address for correspondence: Dr. Gerald I. Cohen, Sinai Hospital, Department of Cardiology, 6767 West Outer Drive, Detroit, Michigan 48235.

0735-1097/96/$15.00
PII S0735-1097(96)00088-5

JACC Vol. 27, No. 7
June 1996:1753–60

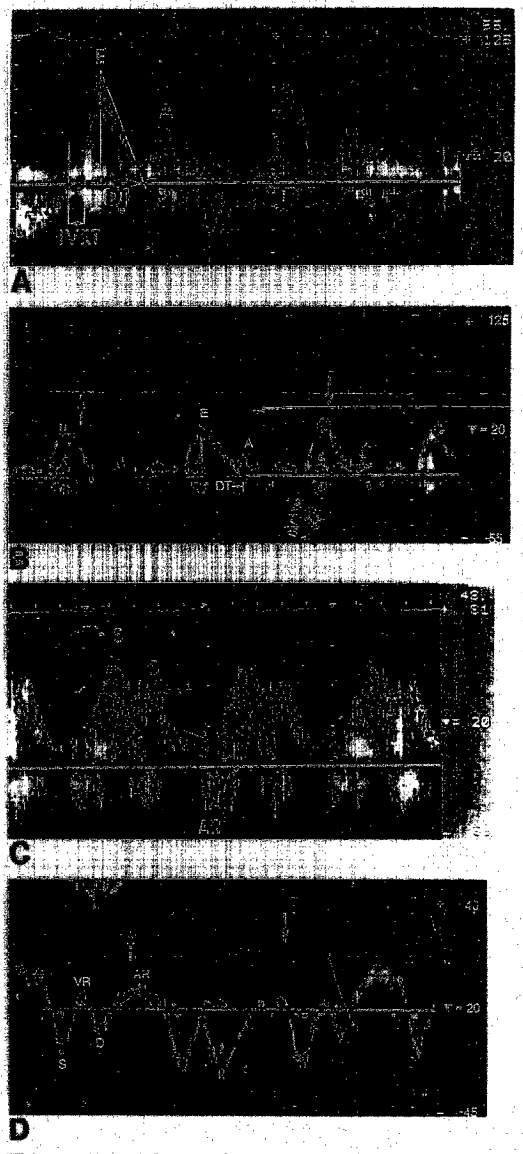

Figure 1. Normal Doppler flow profiles (cm/s) of (A) mitral, (B) tricuspid, (C) pulmonary venous flow and (D) hepatic venous flows. Right-sided flows normally increase with inspiration (↑) and decrease with expiration (↓), although there is little or no respiratory variation in left-sided flows. A = atrial flow velocity; AR = venous flow reversal during atrial contraction; D = diastolic flow velocity; DT = deceleration time; E = early transmitral flow velocity; IVRT = isovolumetric relaxation time; S = systolic flow velocity; VR = venous flow reversal during late ventricular systole.

reversal of pulmonary venous flow during atrial contraction and a venous systolic/diastolic velocity ratio >1 (29,32). On the other hand, healthy young adults without structural heart disease may have a pulmonary venous systolic/diastolic ratio <1 (30,33).

Table 1. Left and Right Ventricular Filling Dynamics in Normal Subjects*

	Age 21–49 yr	Age ≥50 yr
Left ventricular inflow	n = 61	n = 56
Peak E (cm/s)	72 (44–100)	62 (34–90)
Peak A (cm/s)	40 (20–60)	59 (31–87)
E/A ratio	1.9 (0.7–3.1)	1.1 (0.5–1.7)
DT (ms)	179 (139–219)	210 (138–282)
IVRT (ms)	76 (54–98)	90 (56–124)
Pulmonary vein	n = 44	n = 41
Peak S (cm/s)	48 (30–66)	71 (53–89)
Peak D (cm/s)	50 (30–70)	38 (20–56)
S/D ratio	1.0 (0.5–1.5)	1.7 (0.8–2.6)
Peak AR (cm/s)	19 (11–27)	23 (−5–51)
Right ventricular inflow	n = 61	n = 56
Peak E (cm/s)	51 (37–65)	41 (25–57)
Peak A (cm/s)	27 (11–43)	33 (17–49)
E/A ratio	2.0 (1.0–3.0)	1.3 (0.5–2.1)
DT (cm/s)	188 (144–232)	198 (152–244)
Superior vena cava	n = 59	n = 53
Peak S (cm/s)	41 (23–59)	42 (18–66)
Peak D (cm/s)	22 (12–32)	22 (12–32)
Peak AR (cm/s)	13 (7–19)	16 (10–22)

*Normal reference values for Doppler measurements of diastolic function in two age groups of normal subjects. Data presented are mean value (confidence interval). A = atrial flow velocity; AR = venous flow reversal during atrial contraction; D = diastolic flow velocity; DT = deceleration time; E = early transmitral flow velocity; IVRT = isovolumetric relaxation time; S = systolic flow velocity.

Impaired relaxation. Ventricular ischemia, hypertrophy and aging are associated with delay in the energy-dependent reuptake of calcium by the sarcoplasmic reticulum (34–36). Impaired relaxation is typically manifested by Doppler with an E/A ratio <1, an increased deceleration time (typically >220 ms) and an increased isovolumetric relaxation time (typically >100 ms) (Fig. 2, left). An E/A ratio <0.5 is abnormal (30) and may occur when ventricular contraction and relaxation are seriously delayed, prolonged or asynchronous (37). An impaired relaxation pattern also occurs with hypovolemia because of a reduced early transmitral gradient and relatively more ventricular filling during atrial contraction (20,22,38,39).

Pseudonormalization. Pseudonormal filling refers to the normal appearance of ventricular inflow (E/A ratio between 1 and 2; deceleration time between 150 and 220 ms; isovolumetric relaxation time between 60 and 100 ms) in some patients with elevated filling pressures (Fig. 2, center) (32). This pattern represents an intermediate stage between impaired relaxation and restrictive filling as a result of disease progression, ischemia or increased loading conditions (2,14,21,32,40). Reduction of venous return during the Valsalva maneuver causes pseudonormal filling to revert to impaired relaxation (41). Pseudonormal filling is usually indicated by the presence of significant left ventricular or atrial systolic dysfunction or dilation (10).

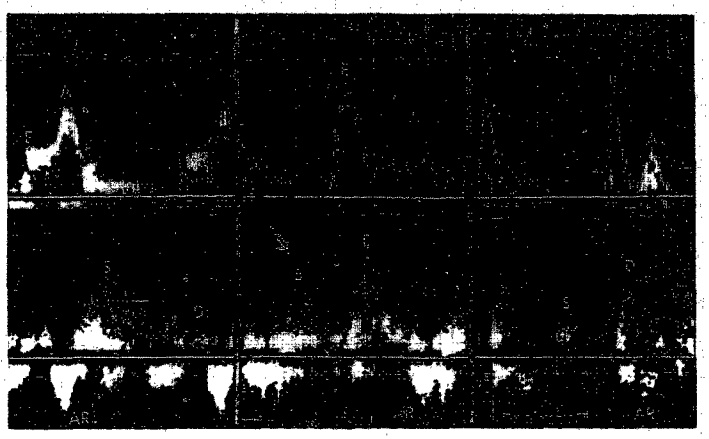

Figure 2. Mitral (**top**) and pulmonary venous (**bottom**) Doppler flow profiles of impaired relaxation (**left**), pseudonormal filling (**center**) and restriction (**right**). Velocity scale markers indicate 20 cm/s. Abbreviations as in Figure 1.

Pulmonary venous flow is usually abnormal. Increased filling pressures are associated with a venous systolic/diastolic ratio <1 (7,9,10). Furthermore, ventricular noncompliance during atrial contraction causes an increased venous flow reversal (>35 cm/s) and termination of transmitral flow before the associated pulmonary venous flow reversal has ended (7,10,32,42). This premature termination of mitral flow predicts a left ventricular end-diastolic pressure >15 mm Hg with an 85% sensitivity and a 79% specificity among patients undergoing diagnostic cardiac catheterization (7).

Restrictive filling. The restrictive filling pattern is characterized by a rapid increase in ventricular pressure during early diastolic filling and little subsequent filling because of chamber stiffness (2,5). Doppler findings consist of an increased E/A ratio (typically >2) and a short deceleration time (typically <150 ms) and isovolumetric relaxation time (typically <60 ms) (Fig. 2, right). In addition, Doppler flows of venous return are greater during diastole than systole (5,43). The momentum of rapid blood flow into the stiff ventricle may cause ventricular pressure to rise quickly and exceed atrial pressure during diastole, reversing the direction of flow and causing *diastolic mitral* and *tricuspid regurgitation* (2,5,32).

Restrictive filling is associated with greater filling pressures, more symptoms and a worsened prognosis (5,11–15). This coincides with more systolic dysfunction and clinical failure among patients with myocardial infarction and idiopathic dilated cardiomyopathy (11–13). In one study of heart failure from ischemic or dilated cardiomyopathy, the mortality rate was 19% at 1 year and 51% at 2 years with restriction (vs. 5% without restriction) (13). Among patients with amyloidosis, wall thickness correlates with disease progression (40). The impaired relaxation pattern of early disease progresses to the restrictive pattern of advanced disease with an associated increase in right (>7 mm) and left (>15 mm) ventricular wall thickness (44,45). When mitral deceleration time decreases to <150 ms, the 1-year survival rate has dropped from 92% to 49% ($p < 0.001$) (14).

Increased respiratory variation. Respiration normally produces little change (<10%) in mitral flow and mild change (<30%) in tricuspid flow (4,6,46). With inspiration, tricuspid flow increases and mitral flow decreases. With expiration, the opposite occurs. Respiratory variation of Doppler flows may be helpful in diagnosing constrictive pericarditis and tamponade.

Constrictive pericarditis. Constrictive pericarditis and restrictive cardiomyopathy may be difficult to distinguish, especially if both are present. Similarities include a short deceleration time or a "dip and plateau" hemodynamic pattern (43,47,48) (Fig. 3A). Differences include increased variation in mitral (≥25%) and pulmonary venous flows during respiration (4,43,48) with constriction but not restriction. Systolic anterograde venous flow is greater in constrictive pericarditis than in restrictive cardiomyopathy (43). Increased flow reversals of hepatic venous flow occur during expiration with constriction and during inspiration with restriction (5,48).

In a study of 25 patients with surgically proven constriction (48), Doppler indicated constriction in 22 (sensitivity 88%) and restriction in 3. A mitral deceleration time <160 ms and an E/A ratio >1 were usually but not always present. The velocity of hepatic venous forward flow during systole equalled or exceeded the diastolic velocity in half of the patients. After pericardiectomy, persistent restrictive filling was associated with less improvement of symptoms (48).

Cardiac tamponade. Cardiac tamponade is associated with respiratory variation in systolic blood pressure (pulsus paradoxus) and Doppler flows (Fig. 3B). This may be due to shielding of the heart (but not the extrapericardial veins) from the normal respiratory variation in intrathoracic pressure. Respiratory variation in the gradient between the pulmonary veins and left atrium results in variation of venous return and left ventricular preload (6,49). Increased chamber coupling with tamponade may also be a cause of respiratory variation of

JACC Vol. 27, No. 7
June 1996:1753–60

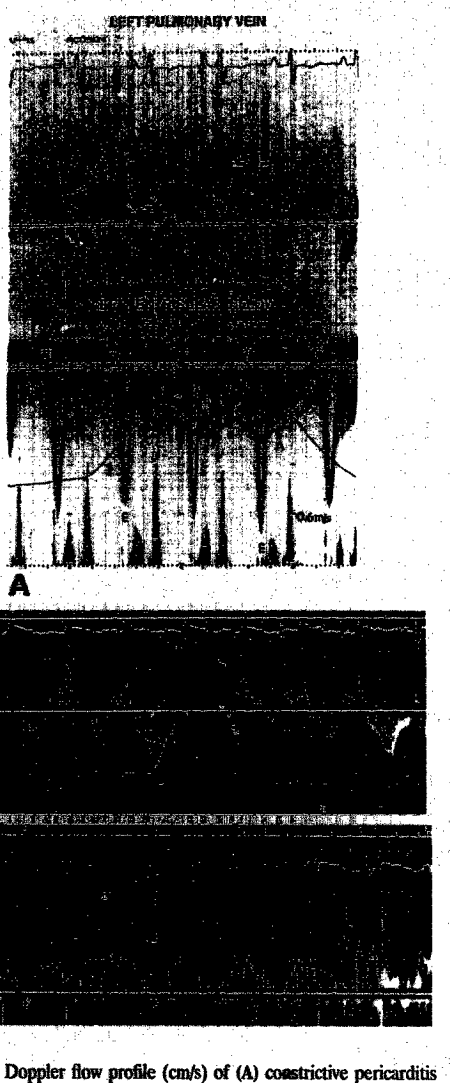

Figure 3. Doppler flow profile (cm/s) of (A) constrictive pericarditis during transesophageal echocardiography and (B) hepatic venous (top) and mitral (bottom) flows in tamponade during transthoracic echocardiography. Increased respiratory variation of flows is present for both diseases. ↑ = inspiration; ↓ = expiration; abbreviations as in Figure 1. Part A is reprinted, with permission, from Klein et al. (43).

Doppler flows and blood pressure. With tamponade, the cardiac chambers are confined to a fixed, noncompliant pericardial space. Increased right heart filling with inspiration can occur only with decreased filling on the left side (50,51). Venous return can only occur when net intrapericardial pressure falls during systolic ejection of blood into the great arteries (52).

Tamponade manifests as a spectrum of clinical and Doppler

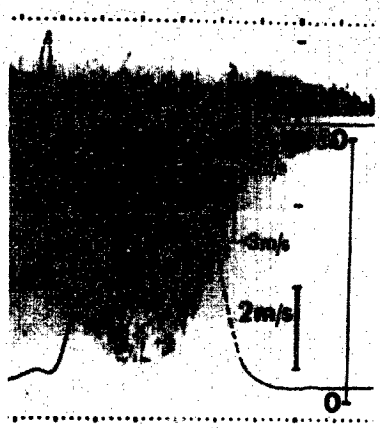

Figure 4. Simultaneous mitral regurgitation Doppler velocity curve and high fidelity left ventricular pressure curve. The time interval (t) from 3 to 1 m/s on the Doppler velocity curve is shown. The time constant of relaxation (tau) is calculated from the left ventricular pressure curve by using a semilogarithmic model from peak negative dP/dt to 5 mm Hg above the left ventricular end-diastolic pressure (**interrupted line**). Pressure calibration is shown from 0 to 150 mm Hg; the Doppler calibration of 2 m/s is also shown. Reprinted, with permission, from Nishimura et al. (3). Copyright © 1993 by the American Heart Association.

echocardiographic findings that complement each other in establishing this diagnosis (52–54). Increased respiratory variation of mitral flow suggests equalization of right-sided pressures and helps indicate the presence of tamponade among patients with large effusions and chamber collapse (54).

Doppler imaging may also distinguish tamponade and constrictive pericarditis, although the two entities may be combined as effusive-constrictive disease (55). Both physiologic findings have increased chamber coupling, pericardial shielding and increased respiratory variation of Doppler flows. However, diastolic venous return is blunted or reversed with tamponade (6,46) and present with constriction (43,47,56). Deceleration time is often shortened with constriction but not with tamponade.

Patients with lung disease may also have increased variation of Doppler flows, although respiration has a relatively delayed impact on mitral and tricuspid flow. In contrast, the greatest increase in tricuspid and mitral flow in constrictive pericarditis and tamponade occurs during the first beat after the onset of inspiration and expiration, respectively (4,6).

Role of transesophageal echocardiography. Transesophageal echocardiography should be considered when the cause, prognosis and optimal treatment of heart failure or hemodynamic instability are not clear from clinical and transthoracic data alone, especially when an operation is being considered. Although transesophageal echocardiography can usually be used to evaluate most Doppler flows, it is especially useful for pulmonary venous flow in the determination of left ventricular pressure and compliance (7,19). In addition, transesophageal

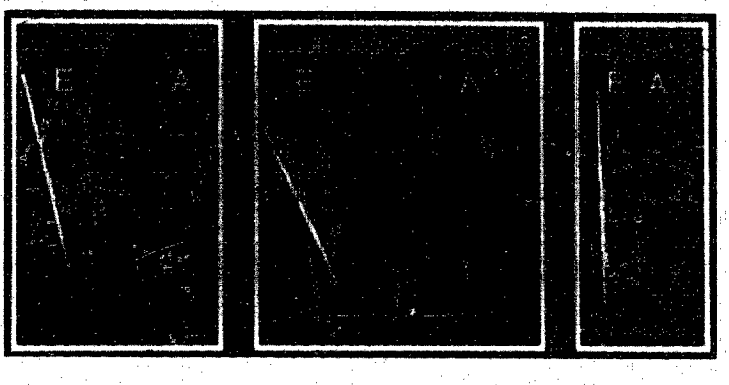

Figure 5. Color Doppler M-mode transesophageal echocardiography of diastolic flow from the left atrium **(top)** toward the ventricular apex **(bottom)**, as imaged in a four-chamber view. Flow propagation is seen during early (E) and late (A) filling with normal filling **(left)**, restriction **(center)** and constriction **(right)**. The E wave maximal velocity is closer to the ventricular apex than the A wave because blood is "pulled" into the actively relaxing ventricle in early diastole and "pushed" into the ventricle during atrial contraction. Compared with normal filling, the flow propagation slope **(white line)** is shallow with restriction and steep with constriction. Scale markers indicate 1 cm.

Doppler echocardiography of the left atrial appendage detects analogous E and A wave velocities that relate to atrial and ventricular systolic and diastolic function (57).

Future Directions

Continuous wave Doppler echocardiography. Continuous wave Doppler echocardiography of mitral and aortic regurgitation during the isovolumetric relaxation period can be used to calculate a measurement of active relaxation called *tau* (Fig. 4) (3,58–60). This parameter is less influenced by loading conditions and heart rate than other Doppler measurements (3,61). With continuous digitization of the isovolumetric mitral regurgitation signal, the rate of fall of left ventricular pressure, or $-dP/dt$, can be estimated (58). Because the Doppler signal of mitral regurgitation reflects the ventriculoatrial gradient, the left ventricular pressure may be calculated by adding an assumed or measured left atrial pressure (60).

Color Doppler M-mode echocardiography. Color Doppler M-mode echocardiography of ventricular inflow generates an equivalent spectral display of mitral E and A waves (Fig. 5). This flow occurs at a finite velocity called the *propagation velocity*, which is measured from the leading edge of the blood wave on color Doppler M-mode echocardiography (62,63). In that the slope of flow propagation decreases as *tau*, $-dP/dt$ and minimal early diastolic pressure increase (64,65), color Doppler M-mode echocardiography may detect delayed apical filling in heart failure (66) and help distinguish pseudonormal from normal filling (65) and restriction from constriction (67).

Doppler tissue imaging. Pulsed wave and color M-mode Doppler imaging can discern segmental and global diastolic function by displaying the velocity of myocardial motion (Fig. 6) (68–71). When the pulsed Doppler cursor is positioned on the myocardium, early and late apical diastolic motion is detected with an E/A ratio that, like the ventricular inflow velocity ratio, falls with aging (70) and ischemic disease (68). Pulsed Doppler imaging of the mitral annulus may help distinguish constriction and normal physiology, which have rapid early diastolic annular motion, from restrictive (and possibly pseudonormal) filling, which has slow annular motion (72).

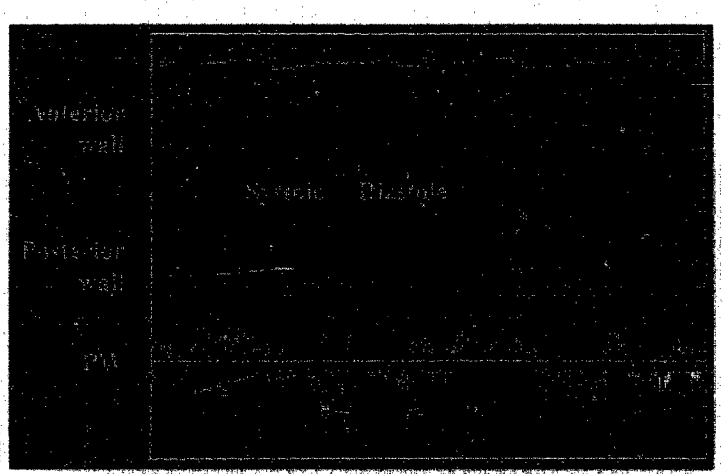

Figure 6. Combination of Doppler tissue imaging and color Doppler M-mode echocardiography of the parasternal short axis **(above)** and pulsed wave (PW) Doppler imaging of the posterior wall **(below)**. Motion toward the transducer is above the pulsed wave Doppler baseline **(color coded red)** and is illustrated by systolic (S) posterior wall motion. Motion away from the transducer is below the pulsed Doppler baseline **(color coded blue)** and is illustrated by diastolic early (E) and late (A) posterior wall motion.

Table 2. Potential Treatment Strategies of Diastolic Function According to Doppler Filling Pattern and Clinical and Two-Dimensional Echocardiographic Context

Doppler Finding	Clinical/Echocardiographic Context	Treatment
Impaired relaxation	Hypovolemia	Fluids
	Excessive afterload	Antihypertensive drugs to regress hypertrophy; relieve outflow obstruction
	Coronary artery disease	Antianginal drugs; revascularization
	Infiltrative cardiomyopathy	Nitrates; diuresis; treat metabolic or immunologic derangement
(E, A wave fusion)	Inadequate filling time	Slow heart rate (beta-blockers, verapamil, diltiazem)
Pseudonormal filling or restriction	Volume overload	Nitrates; diuresis; dialysis; correct valvular regurgitation
	Coronary artery disease	Antianginal drugs; revascularization; transplantation
	Infiltrative cardiomyopathy	Nitrates; diuresis; treat metabolic or immunologic derangement; transplantation
	Dilated cardiomyopathy	Reduce afterload; ACE inhibitors; correct outflow obstruction; optimize preload; treat coronary artery disease; inotropes for systolic dysfunction; transplantation
(end-diastolic MR)	Prolonged PR interval	Dual-chamber pacing to reduce PR interval
Constriction	Thickened pericardium; chamber compression	Medical treatment of cause, especially if acute (antibiotics, anti-inflammatory agents, hormonal therapy, chemotherapy, radiotherapy); pericardial stripping, if chronic
Tamponade	Pericardial effusion; chamber compression	Pericardiocentesis; pericardial window if recurrence likely; medical treatment of cause; evacuate hematoma after heart surgery or rupture; achieve hemostasis

ACE = angiotensin-converting enzyme; MR = mitral regurgitation; other abbreviations as in Table 1.

Limitations and Conclusions

Doppler evaluation of diastolic function may be confounded by an inadequate acoustic window, valvular disease, tachycardia, arrhythmias, suboptimal machine settings and incorrect positioning of the Doppler cursor (73). Although new Doppler methods await establishment of their clinical utility, current techniques are useful in patient management (Table 2) (74–77) because they help diagnose the cause of exercise intolerance, dyspnea, edema and hypoperfusion.

We thank Neil L. Greenberg, MS for contributing Figure 6 to the manuscript.

References

1. Kaul S. Doppler echocardiography in critically ill cardiac patients. Cardiol Clin 1991;9:711–32.
2. Appleton CP, Hatle LK, Popp RL. Relation of transmitral flow velocity patterns to left ventricular diastolic function: new insights from a combined hemodynamic and Doppler echocardiographic study. J Am Coll Cardiol 1988;12:426–40.
3. Nishimura RA, Schwartz RS, Tajik AJ, Holmes DR. Noninvasive measurement of rate of left ventricular relaxation by Doppler echocardiography: validation with simultaneous cardiac catheterization. Circulation 1993;88: 146–55.
4. Hatle LK, Appleton CP, Popp RL. Differentiation of constrictive pericarditis and restrictive cardiomyopathy by Doppler echocardiography. Circulation 1989;79:357–70.
5. Appleton CP, Hatle LK, Popp RL. Demonstration of restrictive ventricular physiology by Doppler echocardiography. J Am Coll Cardiol 1988;11:757–68.
6. Appleton CP, Hatle LK, Popp RL. Cardiac tamponade and pericardial effusion: respiratory variation in transvalvular flow velocities studied by Doppler echocardiography. J Am Coll Cardiol 1988;11:1020–30.
7. Rossvoll O, Hatle LK. Pulmonary venous flow velocities recorded by transthoracic Doppler ultrasound: relation to left ventricular diastolic pressures. J Am Coll Cardiol 1993;21:1687–96.
8. Mulvagh S, Quinones MA, Kleiman NS, Cheirif J, Zoghbi WA. Estimation of left ventricular end-diastolic pressure from Doppler transmitral flow velocity in cardiac patients independent of systolic performance. J Am Coll Cardiol 1992;20:112–9.
9. Kuecherer HF, Muhiudeen IA, Kusumoto FM, et al. Estimation of mean left atrial pressure from transesophageal pulsed Doppler echocardiography of pulmonary venous flow. Circulation 1990;82:1127–39.
10. Appleton CP, Galloway JM, Gonzalez MS, Gaballa M, Basnight MA. Estimation of left ventricular filling pressures using two-dimensional and Doppler echocardiography in adult patients with cardiac disease. J Am Coll Cardiol 1993;22:1972–82.
11. Oh JK, Zee PD, Gersh BJ, Bailey KR, Tajik AJ. Restrictive left ventricular diastolic filling identifies patients with heart failure after acute myocardial infarction. J Am Soc Echocardiogr 1992;5:497–503.
12. Pinamonti B, Di Lenarda A, Sinagra G, Camerini F. Restrictive left ventricular filling pattern in dilated cardiomyopathy assessed by Doppler echocardiography: clinical, echocardiographic and hemodynamic correlations and prognostic implications. J Am Coll Cardiol 1993;22:808–15.
13. Xie GY, Berk MR, Smith MD, Gurley JC, DeMaria AN. Prognostic value of Doppler transmitral flow patterns in patients with congestive heart failure. J Am Coll Cardiol 1994;24:132–9.
14. Klein AL, Hatle LK, Taliercio CP, et al. Prognostic significance of Doppler measures of diastolic function in cardiac amyloidosis. Circulation 1991;83: 808–16.
15. Vanoverschelde JLJ, Raphael DA, Robert AR, Cosyns JR. Left ventricular filling in dilated cardiomyopathy: relation to functional class and hemodynamics. J Am Coll Cardiol 1990;15:1288–95.
16. Keren G, Sonnenblick EH, LeJemtel TH. Mitral anulus motion. Relation to pulmonary venous and transmitral flows in normal subjects and in patients with dilated cardiomyopathy. Circulation 1988;78:621–9.
17. Keren G, Bier A, Sherez J, Miura D, Keefe D, LeJemtel T. Atrial contraction is an important determinant of pulmonary venous flow. J Am Coll Cardiol 1986;7:692–5.
18. Keren G, Sherez J, Megidish R, Levitt B, Laniado S. Pulmonary venous flow pattern—its relationship to cardiac dynamics. A pulsed Doppler echocardiographic study. Circulation 1985;71:1105–12.
19. Nishimura RA, Abel MD, Hatle LK, Tajik AJ. Relation of pulmonary vein to mitral flow velocities by transesophageal Doppler echocardiography: effect of different loading conditions. Circulation 1990;81:1488–97.
20. Nishimura RA, Abel MD, Housmans PR, Warnes CA, Tajik AJ. Mitral flow velocity curves as a function of different loading conditions: evaluation by

intraoperative transesophageal Doppler echocardiography. J Am Soc Echocardiogr 1989;2:79–87.
21. Ishida Y, Meisner JS, Tsujioka K, et al. Left ventricular filling dynamics: influence of left ventricular relaxation and left atrial pressure. Circulation 1986;74:187–96.
22. Greenberg B, Chatterjee K, Parmley WW, Werner JA, Holly AN. The influence of left ventricular filling pressure on atrial contribution to cardiac output. Am Heart J 1979;98:742–51.
23. Vancheri F, Gibson D. Relation of third and fourth heart sounds to blood velocity during left ventricular filling. Br Heart J 1989;61:144–8.
24. Castello R, Pearson AC, Lenzen P, Labovitz AJ. Evaluation of pulmonary venous flow by transesophageal echocardiography in subjects with a normal heart: comparison with transthoracic echocardiography. J Am Coll Cardiol 1991;18:65–71.
25. Appleton CP, Hatle LK, Popp RL. Superior vena cava and hepatic vein Doppler echocardiography in healthy adults. J Am Coll Cardiol 1987;10: 1032–9.
26. Ochi H, Izumi S, Murakami R, Shimada T, Morioka S, Moriyama K. Superior vena cava flow and tricuspid annular motion after cardioversion of atrial fibrillation, and role of right atrial relaxation on systolic venous return. Am J Cardiol 1991;68:1335–9.
27. Klein AL, Stewart WJ, Bartlett J, et al. Effects of mitral regurgitation on pulmonary venous flow and left atrial pressure: an intraoperative transesophageal echocardiographic study. J Am Coll Cardiol 1992;20:1345–52.
28. Klein AL, Cohen GI. Doppler echocardiographic assessment of constrictive pericarditis, cardiac amyloidosis, and cardiac tamponade. Cleve Clin J Med 1992;59:278–90.
29. Klein AL, Tajik AJ. Doppler assessment of pulmonary venous flow in healthy subjects and in patients with heart disease. J Am Soc Echocardiogr 1991;4:379–92.
30. Klein AL, Burstow DJ, Tajik AJ, Zachariah PK, Bailey KR, Seward JB. Effects of age on left ventricular dimensions and filling dynamics in 117 normal persons. Mayo Clin Proc 1994;69:212–24.
31. Pearson AC, Gudipati CV, Labovitz AJ. Effects of aging on left ventricular structure and function. Am Heart J 1991;121:871–5.
32. Appleton CP, Hatle LK. The natural history of left ventricular filling abnormalities: assessment by two-dimensional and Doppler echocardiography. Echocardiography 1992;9:438–57.
33. Citrin BS, Mensah GA, Byrd BF III. Pulmonary vein Doppler flow patterns specific for elevated left ventricular filling pressures in older cardiac patients are common in healthy adults <40 years old. Am J Cardiol 1995;76:730–3.
34. Lakatta EG. Similar myocardial effects of aging and hypertension. Eur Heart J 1990;11 Suppl G:29–38.
35. Nishimura RA, Housmans PR, Hatle LK, Tajik AJ. Assessment of diastolic function of the heart: background and current applications of Doppler echocardiography. Part I. Physiologic and pathophysiologic features. Mayo Clin Proc 1989;64:71–81.
36. Grossman W. Diastolic dysfunction in congestive heart failure. N Engl J Med 1991;325:1557–64.
37. Henein MY, Gibson DG. Suppression of left ventricular early diastolic filling by long axis asynchrony. Br Heart J 1995;73:151–7.
38. Choong CY, Herrmann HC, Weyman AE, Fifer MA. Preload dependence of Doppler-derived indexes of left ventricular diastolic function in humans. J Am Coll Cardiol 1987;10:800–8.
39. Stoddard MF, Pearson AC, Kern MJ, Ratcliff J, Mrosek DG, Labovitz AJ. Influence of alteration in preload on the pattern of left ventricular diastolic filling as assessed by Doppler echocardiography in humans. Circulation 1989;79:1226–36.
40. Klein AL, Hatle LK, Taliercio CP, et al. Serial Doppler echocardiographic follow-up of left ventricular diastolic function in cardiac amyloidosis. J Am Coll Cardiol 1990;16:1135–41.
41. Dumesnil JG, Gaudreault G, Honos GN, Kingma JG. Use of Valsalva maneuver to unmask left ventricular diastolic function abnormalities by Doppler echocardiography in patients with coronary artery disease or systemic hypertension. Am J Cardiol 1991;68:515–9.
42. Appleton CP. Doppler assessment of left ventricular diastolic function: the refinement continues. J Am Coll Cardiol 1993;21:1697–700.
43. Klein AL, Cohen GI, Pietrolungo JF, et al. Differentiation of constrictive pericarditis from restrictive cardiomyopathy by Doppler transesophageal echocardiographic measurements of respiratory variations in pulmonary venous flow. J Am Coll Cardiol 1993;22:1935–43.
44. Klein AL, Hatle LK, Burstow DJ, et al. Comprehensive Doppler assessment of right ventricular diastolic function in cardiac amyloidosis. J Am Coll Cardiol 1990;15:99–108.
45. Klein AL, Hatle LK, Burstow DJ, et al. Doppler characterization of left ventricular diastolic function in cardiac amyloidosis. J Am Coll Cardiol 1989;13:1017–26.
46. Burstow DJ, Oh JK, Bailey KR, Seward JB, Tajik AJ. Cardiac tamponade: characteristic Doppler observations. Mayo Clin Proc 1989;64:312–24.
47. Shabetai R, Fowler NO, Guntheroth WG. The hemodynamics of cardiac tamponade and constrictive pericarditis. Am J Cardiol 1970;26:480–9.
48. Oh JK, Hatle LK, Seward JB, et al. Diagnostic role of Doppler echocardiography in constrictive pericarditis. J Am Coll Cardiol 1994;23:154–62.
49. Golinko RJ, Kaplan N, Rudolph AM. The mechanism of pulsus paradoxus during acute pericardial tamponade. J Clin Invest 1963;42:249–57.
50. Dornhorst AC, Howard P, Leathart GL. Pulsus paradoxus. Lancet 1952;1: 746–8.
51. Shabetai R, Fowler NO, Fenton JC, Masangkay M. Pulsus paradoxus. J Clin Invest 1965;44:1882–98.
52. Gonzalez MS, Basnight MA, Appleton CP. Experimental pericardial effusion: relation of abnormal respiratory variation in mitral velocity to hemodynamics and diastolic right heart collapse. J Am Coll Cardiol 1991;17:239–48.
53. Reddy PS, Curtiss EI, Uretsky BF. The spectrum of hemodynamic changes in cardiac tamponade. Am J Cardiol 1990;66:1487–91.
54. Schutzman JJ, Obarski TP, Pearce GL, Klein AL. Comparison of Doppler and two-dimensional echocardiography for assessment of pericardial effusion. Am J Cardiol 1992;70:1353–7.
55. Hancock EW. Subacute effusive-constrictive pericarditis. Circulation 1971; 43:183–92.
56. Byrd BF, Linden RW. Superior vena cava Doppler flow velocity patterns in pericardial disease. Am J Cardiol 1990;65:1464–70.
57. Kortz RAM, Delemarre BJ, van Dantzig JM, Bot H, Kamp O, Visser CA. Left atrial appendage blood flow determined by transesophageal echocardiography in healthy subjects. Am J Cardiol 1993;71:976–81.
58. Chen C, Rodriguez L, Lethor JP, Levine RA. Continuous wave Doppler echocardiography for noninvasive assessment of left ventricular dP/dt and relaxation time constant from mitral regurgitation spectra in patients. J Am Coll Cardiol 1994;23:970–6.
59. Yamamoto K, Masuyama T, Doi Y, Naito J. Noninvasive assessment of left ventricular relaxation using continuous-wave Doppler aortic regurgitant velocity curve: its comparative value to the mitral regurgitation method. Circulation 1995;91:192–200.
60. Chen C, Rodriguez L, Levine RA, Weyman AE, Thomas JD. Noninvasive measurement of the time constant of left ventricular relaxation using the continuous-wave Doppler velocity profile of mitral regurgitation. Circulation 1992;86:272–8.
61. Weiss JL, Frederiksen JW, Weisfeldt ML. Hemodynamic determinants of the time-course of fall in canine left ventricular pressure. J Clin Invest 1976;58:751–60.
62. Thomas JD, Aragam JR, Rodriguez LL, Adams M, Weyman AE. Spatiotemporal distribution of mitral inflow velocity: use of the color Doppler M-mode echocardiogram to investigate intracardiac pressure gradients [abstract]. Med Biol Eng Comput 1991;29 Suppl 1:130.
63. Thomas JD, Vandervoort PM, Greenberg NL, Ares MA, Adams MS. Application of color Doppler M-mode echocardiography in the assessment of ventricular diastolic function: analysis of the spatiotemporal velocity distribution. In: Ingels NB Jr, editor. Systolic and Diastolic Function of the Heart. (Proceedings of the Cardiovascular System Dynamics Society.) Amsterdam: IOS Press. In press.
64. Brun P, Tribouilloy C, Duval AM, et al. Left ventricular flow propagation during early filling is related to wall relaxation: a color M-Mode Doppler analysis. J Am Coll Cardiol 1992;20:420–32.
65. Takatsuji H, Mikami T, Urasawa K, et al. A new approach for evaluation of left ventricular diastolic function: spatial and temporal analysis of left ventricular filling flow propagation by color M-mode Doppler echocardiography. J Am Coll Cardiol 1996;27:365–71.
66. Stuggard M, Risoe C, Ihlen H, Smiseth OA. Intracavitary filling pattern in the failing left ventricle assessed by color M-mode Doppler echocardiography. J Am Coll Cardiol 1994;24:663–70.

67. Rodriguez L, Ares MA, Vandervoort PM, Thomas JD, Greenberg NL, Klein AL. Does color M-mode flow propagation differentiate between patients with restrictive vs constrictive physiology [abstract]? J Am Coll Cardiol 1996;27 Suppl A:268A.
68. Isaaz K, Thompson A, Ethevenot G, Cloez JL, Brembilla B, Pernot C. Doppler echocardiographic measurement of low velocity motion of the left ventricular posterior wall. Am J Cardiol 1989;64:66–75.
69. Miyatake K, Yamagishi M, Tanaka N, et al. New method for evaluating left ventricular wall motion by color-coded tissue Doppler imaging: in vitro and in vivo studies. J Am Coll Cardiol 1995;25:717–24.
70. Garcia MJ, Rodriguez L, Homa D, et al. Intramyocardial motion assessment by Doppler ultrasound: characteristic findings in normal subjects [abstract]. J Am Soc Echocardiogr 1994;7:S14.
71. Gorcsan J III, Katz WE, Mandarino WA. Heterogeneous left ventricular septal and posterior wall velocities: quantitative temporal assessment by myocardial color Doppler imaging [abstract]. Circulation 1994;90 Suppl I:I-327.
72. Garcia MJ, Rodriguez L, Ares M, Griffin BP, Thomas JD, Klein AL. Differentiation of constrictive pericarditis from restrictive cardiomyopathy: assessment of left ventricular diastolic velocities in longitudinal axis by Doppler tissue imaging. J Am Coll Cardiol 1996;27:108–14.
73. Grodecki PV, Klein AL. Pitfalls in the echo-Doppler assessment of diastolic dysfunction. Echocardiography 1993;10:213–34.
74. Williams JF, Bristow MR, Fowler MB, et al. Guidelines for the evaluation and management of heart failure. Report of the American College of Cardiology/American Heart Association task force on practice guidelines. J Am Coll Cardiol 1995;26:1376–98.
75. Nishimura RA, Hayes DL, Holmes DR, Tajik AJ. Mechanism of hemodynamic improvement by dual-chamber pacing of severe left ventricular dysfunction: an acute Doppler and catheterization hemodynamic study. J Am Coll Cardiol 1995;25:281–8.
76. Brutsaert DL, Sys SU, Gillebert TC. Diastolic failure: pathophysiology and therapeutic implications. J Am Coll Cardiol 1993;22:318–25.
77. Oh JK, Hatle LK, Mulvagh SL, Tajik AJ. Transient constrictive pericarditis: diagnosis by two-dimensional Doppler echocardiography. Mayo Clin Proc 1993;68:1158–64.